OPEN ACCESS Freely available online

PLOS ONE

Discovery of a Novel Target for the Dysglycemic Chromogranin A Fragment Pancreastatin: Interaction with the Chaperone GRP78 to Influence Metabolism

Nilima Biswas[1], Ryan S. Friese[1], Jiaur R. Gayen[1], Gautam Bandyopadhyay[1], Sushil K. Mahata[1,4], Daniel T. O'Connor[2,3,4]*

1 Departments of Medicine, University of California San Diego, La Jolla, California, United States of America, **2** Department of Pharmacology, University of California San Diego, La Jolla, California, United States of America, **3** Institute for Genomic Medicine, University of California San Diego, La Jolla, California, United States of America, **4** VA San Diego Healthcare System, San Diego, California, United States of America

Abstract

Rationale: The chromogranin A-derived peptide pancreastatin (PST) is a dysglycemic, counter-regulatory peptide for insulin action, especially in liver. Although previous evidence for a PST binding protein has been reported, such a receptor has not been identified or sequenced.

Methods and Results: We used ligand affinity to purify the PST target, with biotinylated human PST ($hCHGA_{273–301}$-amide) as "bait" and mouse liver homogenate as "prey", and identified GRP78 (a.k.a. "78 kDa Glucose Regulated Protein", HSPA5, BIP) as a major interacting partner of PST. GRP78 belongs to the family of heat shock proteins (chaperones), involved in several cellular processes including protein folding and glucose metabolism. We analyzed expression of GRP78 in the absence of PST in a mouse knockout model lacking its precursor CHGA: hepatic transcriptome data revealed global over-expression of not only GRP78 but also other heat shock transcripts (of the "adaptive UPR") in CHGA(−/−) mice compared to wild-type (+/+). By contrast, we found a global decline in expression of hepatic pro-apoptotic transcripts in CHGA(−/−) mice. GRP78's ATPase enzymatic activity was dose-dependently inhibited by PST (IC_{50}~5.2 μM). PST also inhibited the up-regulation of GRP78 expression during UPR activation (by tunicamycin) in hepatocytes. PST inhibited insulin-stimulated glucose uptake in adipocytes, and increased hepatic expression of G6Pase (the final step in gluconeogenesis/glycogenolysis). In hepatocytes not only PST but also other GRP78-ATPase inhibitors (VER-155008 or ADP) increased G6Pase expression. GRP78 over-expression inhibited G6Pase expression in hepatocytes, with partial restoration by GRP78-ATPase inhibitors PST, VER-155008, or ADP.

Conclusions: Our results indicate that an unexpected major hepatic target of PST is the adaptive UPR chaperone GRP78. PST not only binds to GRP78 (in pH-dependent fashion), but also inhibits GRP78's ATPase enzymatic activity, and impairs its biosynthetic response to UPR activation. PST decreases insulin-stimulated cellular glucose uptake, and PST as well as other chaperone ATPase activity inhibitors augment expression of G6Pase; GRP78 over-expression antagonizes this PST action. Analysis of the novel PST/GRP78 interaction may provide a new avenue of investigation into cellular glycemic control as well as dysglycemia.

Citation: Biswas N, Friese RS, Gayen JR, Bandyopadhyay G, Mahata SK, et al. (2014) Discovery of a Novel Target for the Dysglycemic Chromogranin A Fragment Pancreastatin: Interaction with the Chaperone GRP78 to Influence Metabolism. PLoS ONE 9(1): e84132. doi:10.1371/journal.pone.0084132

Editor: Alessandro Bartolomucci, University of Minnesota, United States of America

Received September 21, 2013; **Accepted** November 12, 2013; **Published** January 20, 2014

Funding: This work was supported by the National Institutes of Health and the Department of Veterans Affairs. The funders had no role in study design, data collection and analysis, decision to publish, or preparation of the manuscript.

Competing Interests: The authors have declared that no competing interests exist.

* E-mail: doconnor@ucsd.edu

Introduction

Pancreastatin (PST, human $CHGA_{250–301}$-amide) is derived from the proteolytic cleavage of its precursor, chromogranin A (CHGA), an acidic glycoprotein abundant in secretory granules of chromaffin cells and also present throughout the neuroendocrine system [1]. Several processing intermediates have been reported for PST in cells or tissues, and all contained the biologically conserved active carboxyl-terminal part of the molecule [2–5]. The amidated carboxyl terminus of PST is a feature in common with many neuropeptides and gastrointestinal hormones such as NPY and PYY.

The activity of PST as a regulatory gastroenteropancreatic peptide has been established in the light of a variety of biological effects in a number of tissues [6–9], including its role in modulation of energy metabolism, with a general counter-regulatory effect to insulin. PST induces glycogenolysis in liver and lipolysis in adipocytes [10,11]. PST inhibits insulin action in rat adipocytes in a dose dependent manner and within a physiological range of concentration [12] and inhibits both basal and insulin-stimulated glycogen synthesis [13]. Metabolic effects of PST have been confirmed in humans and naturally occurring human variants have been found, such as Gly297Ser in the

functionally important carboxyl terminus of the peptide, substantially increasing its potency to inhibit cellular glucose uptake [14].

Preliminary pharmacological characterization of a PST binding protein has been described in rat liver, hepatoma, adipocytes and heart membranes [15–18]. A putative PST receptor was purified from rat liver membranes by Sanchez-Margalet et al., and may be physically associated with a Gαq/11 protein [19]; however the final identification and sequencing of such a PST receptor have been elusive so far. PST seems to activate a receptor signaling pathway that is typically associated with seven-spanning transmembrane receptors coupled to Gq-PLCβ-calcium-PKC signaling and mediated through protein kinase C and NO-dependent pathways [20–23]. Increased PST plasma levels, correlating with catecholamine levels have been found in insulin resistant states such as gestational diabetes, essential hypertension or type 2 diabetes mellitus [24–27].

In studies by Gayen et al, CHGA knockout (−/−) mice display *enhanced* glycemic control in spite of *low* plasma insulin levels, because of increased liver insulin sensitivity, and treatment of such mice with PST increased blood glucose in association with augmented phosphoenolpyruvate carboxykinase and glucose-6-phosphatase mRNA expression [23]. The pathway from PST towards these effects may include IRS1/2-phosphatidylinositol 3-kinase-AKT-FOXO-1 activation, as well as effects on insulin-induced maturation of SREBP1c by PKC and elevated NO [23].

To understand the earliest stage of PST action, we searched for its cellular interacting partner (or target) by PST-ligand (''bait'') affinity chromatography on liver proteins (''prey''). We found that PST interacts directly with the chaperone GRP78, a widely expressed, ~78-kDa ''Glucose-Regulated Protein'', also known as ''Binding Immunoglobulin Protein'' (BIP) or Heat Shock Protein A5 (HSPA5) [28]. The interaction of GRP78 with PST, and its implications for glucose homeostasis and dysglycemia are explored here.

Experimental Procedures

Ethics statement

The experimental animal (mouse) studies were approved by the UCSD Institutional Animal Care And Use Committee (Protocol S00048M).

Ligand affinity isolation of a PST binding protein

Freshly obtained normal mouse liver was homogenized in cold, freshly prepared buffer (10 mM Hepes, pH 7.4, 0.1 mM EDTA) with a cocktail of protease inhibitors (Protease inhibitor cocktail set III, Calbiochem at 1:100: PMSF 5 mM, benzamidine hydrochloride 50 mg/mL, TLCK [N-Tosyl-Lys Chloromethyl Ketone] hydrochloride 0.1 mM), and centrifuged at 50,000 g for 30 min to pellet crude membranes. The membrane preparation was washed once with the same buffer and then solubilized with 1% v/v Triton X-100 in 25 mM Hepes pH 7.4, 100 mM NaCl, 2 mM $MgCl_2$, 1 mM KCl and protease inhibitor cocktail as mentioned above, for 1 hr at 4°C, then centrifuged at 100,000 g for 1 hr, and the supernatant was saved.

Biotinylated human PST ($hCHGA_{273–301}$-amide) was synthesized by placing a biotin residue at the amino terminus of the peptide, separated by a spacer consisting of four amino acids (EAQD) from the natural sequence: Biotin-EAQD-PEGKGE-QEHSQQKEEEEEMAVVPQGLFRG-amide. A ligand affinity column was prepared by incubating 5 mg of biotin-PST-amide with 1 ml of 50% streptavidin agarose resin (Thermo Scientific) in column buffer (25 mM Hepes, pH 7.4, 100 mM NaCl, 2 mM $MgCl_2$, 1 mM KCl, 1% Triton and protease inhibitor cocktail) for 1 hr at 4°C.

The streptavidin resin was washed extensively with the same buffer and then incubated with solubilized liver membranes for 18 hr at 4°C. The resin was packed into a chromatography column, washed with the column buffer containing 0.1% Triton, and bound proteins were eluted with column buffer adjusted down from pH 7.4 to 5.5. Fractions eluted were concentrated by TCA precipitation and analyzed on 8–16% SDS-PAGE gradient slab gels, stained with coomassie blue G-250 (SimplyBlue Safestain; Invitrogen). The resulting ~75 kDa major protein band was excised, subjected to in-gel digestion with trypsin (see below), and the resulting peptides were separated by reverse-phase liquid chromatography followed by tandem mass spectrometry.

During the original experiment, a minor band of ~175 kDa was also observed, but not characterized further. A similar/control ligand affinity experiment on liver membranes was performed with the CHGA-derived biologically active peptide catestatin (human $CHGA_{352–372}$) as the immobilized biotinylated ligand.

In-gel digest of the PST-binding protein

Gel slices were cut to 1×1 mm cubes and destained 3 times by first washing with 100 µl of 100 mM ammonium bicarbonate for 15 min, followed by addition of 100 µl acetonitrile (ACN) for 15 min. The gel pieces were then dried in a SpeedVac and reduced by mixing with 200 µl of 100 mM ammonium bicarbonate-10 mM DTT by incubating at 56°C for 30 min. The liquid was removed and 200 µl of 100 mM ammonium bicarbonate/55 mM iodoacetamide was added to gel pieces and incubated at room temperature in the dark for 20 min. After the removal of the supernatant and one wash with 100 mM ammonium bicarbonate for 15 min, the same volume (200 µl) of ACN was added to dehydrate the gel pieces. The solution was then removed and samples were vacuum-dried (SpeedVac). For digestion, enough solution of ice-cold trypsin (0.01 µg/µl) in 50 mM ammonium bicarbonate was added to cover the gel pieces and set on ice for 30 min. After complete rehydration, excess trypsin solution was removed, replaced with fresh 50 mM ammonium bicarbonate, and left overnight at 37°C. The peptides were extracted twice by addition of 50 µl of 0.2% formic acid and 50% ACN, and vortex-mixed at room temperature for 30 min. The combined extractions were analyzed directly by reverse-phase liquid chromatography (LC) in combination with tandem mass spectroscopy (MS/MS) using electrospray ionization [29].

LC-tandem-MS/MS analysis

Proteins extracted from SDS-PAGE gels and trypsin-digested were analyzed by liquid chromatography (LC, C-18)-tandem-MS/MS with electrospray ionization. Nanospray ionization experiments were performed with a QSTAR-Elite hybrid mass spectrometer (AB/MDS Sciex) interfaced to a nanoscale reverse-phase high-pressure liquid chromatograph (Tempo) with a 10 cm-180 micron ID glass capillary packed with 5-µm C-18 Zorbax™ beads (Agilent). The buffer compositions were as follows. Buffer A was composed of H_2O containing 2% ACN, 0.2% formic acid, and 0.005% TFA; buffer B was composed of 100% ACN containing 0.2% formic acid, and 0.005% TFA. Peptides were eluted from the C-18 column into the mass spectrometer using a linear gradient of 5–60% buffer B over 60 min at 400 µl/min. LC-MS/MS data were acquired in peak-dependent fashion by selecting the 4 most intense peaks with charge state of +2 to +4 that exceeds 20 counts, with exclusion of former target ions set to ''360 sec'' and mass tolerance for exclusion set to 100 ppm. Time-of-Flight (TOF) MS data were acquired at m/z 400 to 1600 Da,

while MS/MS data were acquired from m/z 50 to 2,000 Da. Peptide identifications were made using the Paragon algorithm executed in Protein Pilot 2.0 (Life Technologies).

Plasmids

The human G6P-ase promoter-luciferase reporter plasmid has been described [23]. The GRP78 (BIP) promoter-luciferase reporter was a gift from Bruce M. Spiegelman (Harvard Medical School). The pCMV promoter-driven human GRP78 (HSPA5) expression plasmid was from Origene <www.origene.com/>. pSV-Beta-Gal (a transfection efficiency control plasmid, in which the SV40 early promoter drives expression of beta-galactosidase) was obtained from Promega <www.promega.com>.

GRP78's ATPase enzymatic activity

Concentration-dependent spectrophotometric assays were carried out using recombinant human GRP78 protein (catalog # ab78432, Abcam Inc., Cambridge, MA) at concentrations of 0.063, 0.125, 0.25 and 0.5 μM in 50 μl of assay buffer (20 mM Tris, pH 7.5, 50 mM KCl, 1.5 mM $MgCl_2$). The reaction was started by adding 100 μM ATP and incubated for 37°C for 30 min. Liberated free phosphate (Pi) was measured by a Malachite green-phosphate assay (catalog #10009325, Cayman <https://www.caymanchem.com>). The assay method is based on formation of a complex between malachite green molybdate and Pi (free orthophosphate) that absorbs at 620–640 nm. Assays to determine inhibition of ATPase activity were done with GRP78 (0.25 μM), with or without PST (0 to 10 μM).

Transfection and luciferase reporter activity of human HepG2 hepatocytes

Cells were plated on 24 well tissue culture plates the day before transfection. 0.5 to 1.0 μg of total DNA per well was used for transfection with Transfectin (BioRad). In some experiments, pSV-Beta-Gal (Promega; in which the SV40 early promoter drives expression of beta-galactosidase) was co-transfected as a transfection efficiency control. After 5 hrs supernatants were removed and fresh media containing different compounds as mentioned in the respective figures were added. 18 hrs after transfection, supernatants were removed and cells were lysed in passive lysis buffer (Promega) and the luciferase and beta-galactosidase activity were measured. Luciferase activity was normalized by beta-galactosidase as well as cellular protein, determined by dye-binding (coomassie G-250; BioRad).

Transcriptome of liver and adrenal gland in organisms with (CHGA[+/+]) or without (CHGA[−/−]) a functional CHGA gene

Genome-wide transcriptome profiling in CHGA knockout (−/−, CHGA KO) and wild-type (+/+, WT) mice (n = 3 biological replicates each) was measured in mRNA from the adrenal gland or liver, by Affymetrix GeneChip hybridization (MG-U74Av2 GeneChips for adrenal glands; Mouse 430A 2.0 GeneChips for livers), as described [30]. Pathway analyses, by functional clustering, were conducted with the NCI-DAVID (**D**atabase for **A**nnotation, **V**isualization and **I**ntegrated **D**iscovery) package, at <http://david.abcc.ncifcrf.gov/>. The DAVID algorithm addresses the redundant nature of genomic annotation that tends to dilute biological meaning during interpretation of gene expression data and is based on the hypothesis that similar functional annotations should have similar gene members. DAVID functional annotation clustering integrates kappa statistics and fuzzy heuristic clustering to group similar annotations into functional clusters. The P value associated with each annotation term is a modified Fisher exact score. The functional cluster enrichment score is the $-\log_{10}$ transformation of the geometric mean of all annotation terms within the functional cluster. Clusters are selected from Gene Ontology functional groups (GO at <http://amigo.geneontology.org>)

3T3-L1 pre-adipocytes: Culture and differentiation

3T3-L1 mouse pre-adipocytes from ZenBio <www.zen-bio.com> were cultured and differentiated to the adipocyte phenotype following the protocol from the manufacturer, in which adipocyte differentiation occurs in response to 3-isobutyl-1-methylxanthine (IBMX 500 μM), dexamethasone (1 μM), and insulin (1.7 μM).

Measurement of cellular glucose uptake by adipocytes

Differentiated 3T3-L1 adipocytes cultured in 24-well plate were washed once with DMEM low glucose serum free medium and then serum-starved (serum free medium with 0.5% fatty acid-free BSA) for an additional 3 hrs, washed three times with Hepes/salts buffer (25 mM Hepes, pH 7.4, 120 mM NaCl, 5 mM KCl, 1.2 mM $MgSO_4$, 1.3 mM $CaCl_2$, 1.3 mM KH_2PO_4) and then incubated in the same buffer at 37°C. Subsequently the cells were stimulated with or without 100 nM insulin in the presence or absence of PST (100 nM) for 30 min, and 2-deoxy-D-[^{3}H]glucose was added during the last 10 min at a final concentration of 100 μM (specific activity: 0.2 μCi/ml). Glucose uptake was terminated by washing three times with ice-cold PBS, and the cells were then lysed with 1 N NaOH for 30 min, neutralized and subjected to liquid scintillation counting.

Statistics

Results are expressed as mean ± SEM. Inter-group comparisons were made by t test, 1-way or 2-way ANOVA, as appropriate, in Kaleidagraph <www.synergy.com>.

Results

PST binds liver target GRP78 (HSPA5, BIP) in pH-dependent fashion

To identify novel proteins that interact with PST, we used affinity chromatography with biotinylated human PST-amide and a murine liver homogenate, eluting the bound protein by lowering pH from 7.4 to 5.5, followed by analysis with LC-tandem-MS/MS mass spectrometry. The major protein band detected after coomassie blue staining had M_r ~75 kDa (Fig. 1A). When subjected to trypsin digestion and LC-MS/MS analysis, the band was identified as GRP78 (BIP, HSPA5; Fig. 1, Table 1, Table S1), with 44 spectra spanning ~66% of the GRP78 amino acid sequence (Fig. 1C). The target seemed to be full-length mouse GRP78 (rather than the cytosolic splice variant GRP78va [31]) since at the amino terminus the identified peptide extended up to (but not including) the 19-amino acid signal peptide (MMKFTVVAAALLLLGAVRA), while at the carboxy-terminus the identified peptides spanned KD of the KDEL retention signal.

Tryptic peptides from two other heat shock family proteins, stress 70 protein (GRP75, HSPA9) and heat shock cognate 71 kDa protein (HSPA8) were also identified, with overall rank order of abundance: 1>2>3 = GRP78>GRP75>HSPA8 (Table 1 & Table S1). In addition we noted trace quantities of typically observed peptides from trypsin and keratin.

Affinity chromatography with another CHGA derived peptide catestatin (human $CHGA_{352–372}$) on liver homogenate did not pull

A.

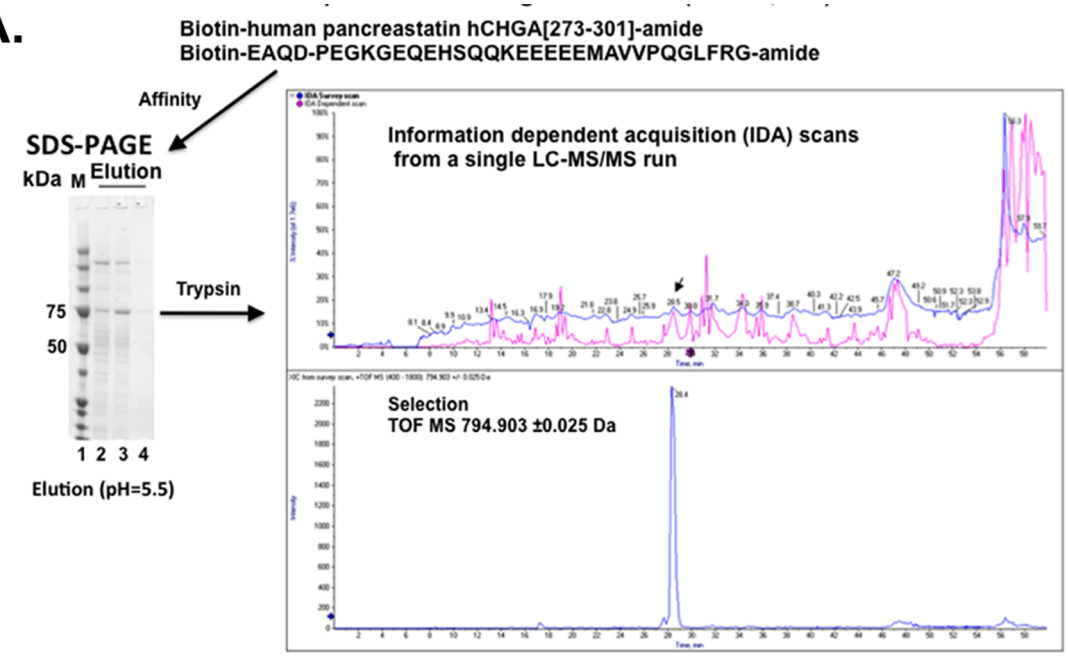

B.

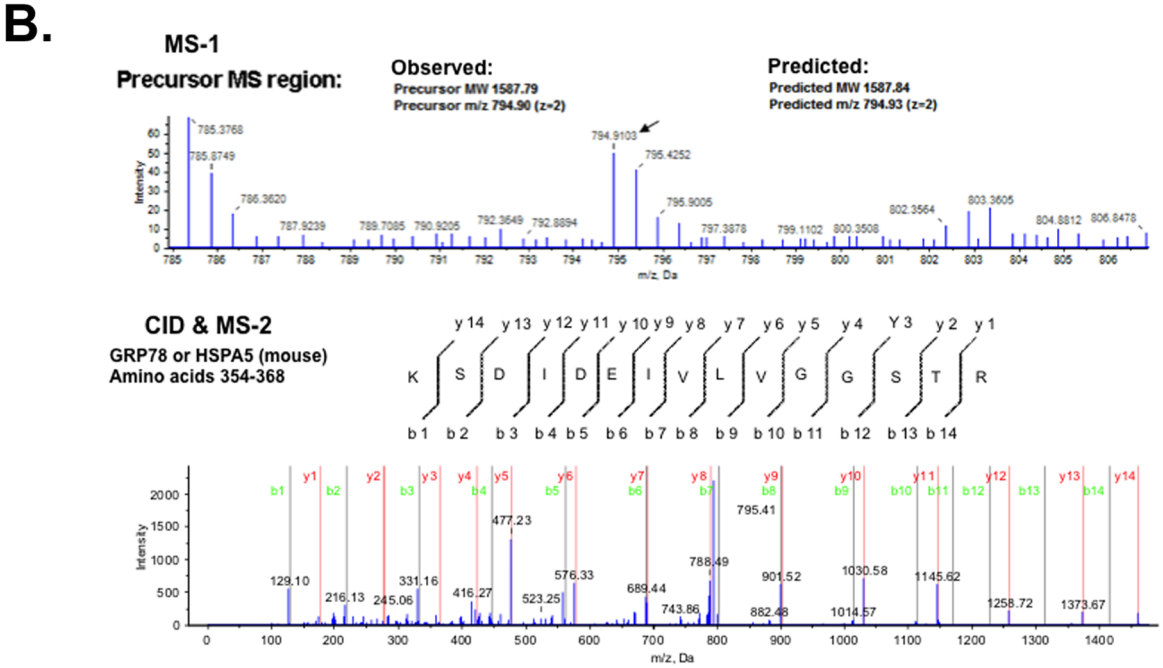

C.

Identification of GRP78 (HSPA5) after PST affinity elution: Peptide coverage during LC-MS/MS. The map was generated from target MS/MS fragment sequences in Protein Pilot 2.0 (Life Technologies).; Peptides identified with at least 95% confidence are in **bold** type. Template: UniProtKB P20029 (GRP78_MOUSE).

Mouse GRP78 (minus 19-aa signal peptide):

EEEDKKEDVGTVVGIDLGTTYSCVGVFKNGRVEIIANDQGNRITPSYVAFTPEGERLIGD
AAK**NQLTSNPENTVFDAKR**LIGR**TWNDPSVQQDIK**FLPFKVVEK**KTKPYIQVDIGGGQTK**
TFAPEEISAMVLTKMKETAEAYLGKKVTHAVVTVPAYFNDAQRQATK**DAGTIAGLNVMRI**
INEPTAAAIAYGLDKREGEKNILVFDLGGGTFDVSLLTIDNGVFEVVATNGDTHLGGEDF
DQRVMEHFIKLYKKKTGKDVRKDNRAVQKLRREVEKAKRALSSQHQAR**IEIESFFEGEDF**
SETLTRAKFEELNMDLFRSTMKPVQKVLEDSDLK**KSDIDEIVLVGGSTR**IPKIQQLVKEF
FNGKEPSR**GINPDEAVAYGAAVQAGVLSGDQDTG**DLVLLDVCPLTLGIETVGGVMTKLIP
RNTVVPTK**KSQIFSTASDNQPTVTIKVYEGERPLTKDNHLLGTFDLTGIPPAPR**GVPQIE
VTFEIDVNGILRVTAEDKGTGNKNKITITNDQNRLTPEEIERMVNDAEKFAEEDKKLKER
IDTR**NELESYAYSLK**NQIGDKEKLGGKLSSEDKETMEKAVEEK**IEWLESHQDADIEDFKA**
KKKELEEIVQPIISKLYGSGGPPPTGEEDTSEKDEL

Figure 1. Identification of a PST binding protein from mouse liver membranes: Isolation and identification. (1A) and (1B) Affinity chromatography followed by LC-tandem-MS/MS. (**1A**): **SDS-PAGE separation, followed by trypsin digestion and C-18 liquid chromatography**. The mouse liver homogenate was subjected to ligand affinity chromatography using a biotinylated human pancreastatin ($hCgA_{273–301}$-amide) peptide as "bait". Triton-solubilized liver membranes (as "prey") were incubated with bio-PST, which was pre-incubated with streptavidin agarose. Bound proteins were eluted by lowering pH to 5.5, and analyzed by SDS-PAGE. Gel lanes: 1 = Protein size standards; 2–4 = serial fractions during elution at lower pH = 5.5. The major ~75 kDa band was excised from the gel and subjected to trypsin digestion, and the resulting peptides were separated by liquid chromatography (chromatogram shown above). Selection (arrow) of a peak for further analysis is also shown. (**1B**): **First and second dimensions of MS, with sequence identification**. The first dimension of MS is displayed above. In the second dimension of MS, one ion is chosen (arrow), and a representative MS/MS spectrum of mouse $GRP78_{354–368}$ is shown. (**1C**): **Identification of GRP78 (HSPA5) after PST affinity elution: Peptide coverage during LC-MS/MS**. The map was generated from target MS/MS fragment sequences in Protein Pilot 2.0 (Life Technologies).; Peptides identified with at least 95% confidence are in **bold** type. Template: UniProtKB P20029 (GRP78_MOUSE).
doi:10.1371/journal.pone.0084132.g001

down the GRP78 protein, as evidenced by the SDS-PAGE and subsequent LC-MS/MS analysis (results not shown).

Liver and adrenal expression of endogenous GRP78, and other UPR components (adaptive and pro-apoptotic), in the absence of CHGA (i.e., CHGA[−/−] mice)

The CHGA KO mouse displays *enhanced* glycemic control, with normal plasma glucose even in the face of reduced plasma insulin [23,30]. To explore the role of CHGA as well as CHGA-derived PST, we profiled the liver transcriptome in CHGA +/+ versus −/− mice. Liver expression of GRP78 increased by +44% (−/− > +/+: p = 6.28E-05; 2 probes) in CHGA KO mice compared to wild-type (WT) (Fig. 2A), though not in adrenal gland.

Pathway analyses by the NCI-DAVID algorithms indicated global dysregulation of UPR pathway gene expression in liver of CHGA +/+ versus −/− mice. The peak pathway association was at Gene Ontology term GO:0006986 ("Response to unfolded protein"; genes: MM.378901, MM.31102, MM.390966, MM.4068, MM.271160, MM.24192, MM.43745, MM.10353, MM.247167, MM.440064, MM.18845, MM.2161, MM.341186, MM.29778, MM.387108, MM.28131, MM.56895, MM.29524, MM.289387, MM.110220, MM.142843, MM.260456, MM.29702, MM.378990, MM.275309, MM.273049, MM.55422, MM.39330, MM.1457, MM.149870, MM.4048, MM.340943, MM.28420, MM.24174, MM.1025, MM.293321, MM.294693, MM.27445, MM.29151, MM.20452, MM.299952, MM.217616, MM.337691, MM.42163, MM.12616, MM.169929, MM.391651, MM.21596, MM.240327, MM.653, MM.317701). The DAVID fold-enrichment score for the overall UPR pathway was 103.9 (p = 1.41E-130), with Bonferroni

Table 1. PST binding protein summary statistics.

Rank	% Coverage	Accession	Name	Peptides (>95% conf)
1	66.11	gi|254540168	78 kDa glucose-regulated protein precursor [Mus musculus]	44
2	60.09	gi|162461907	stress-70 protein, mitochondrial [Mus musculus]	47
3	59.75	gi|31981690	heat shock cognate 71 kDa protein [Mus musculus]	17
4	28.18	gi|31560705	long-chain-fatty-acid–CoA ligase 1 [Mus musculus]	11
5	53.25	gi|84781771	trypsin 10 [Mus musculus]	2
6	8.32	gi|126116585	keratin, type II cytoskeletal 1 [Mus musculus]	3
7	16.22	gi|112983636	keratin, type I cytoskeletal 10 [Mus musculus]	2
8	14.57	gi|71043961	trypsinogen 7 [Mus musculus]	3
9	5.78	gi|113195684	keratin, type II cytoskeletal 6B [Mus musculus]	2
10	26.42	gi|6755893	trypsin 4 [Mus musculus]	3
11	7.49	gi|239787090	peroxisomal acyl-coenzyme A oxidase 2 [Mus musculus]	1
12	22.03	gi|51092293	keratin, type II cytoskeletal 1b [Mus musculus]	2
13	12.80	gi|47059013	keratin, type II cytoskeletal 73 [Mus musculus]	2
14	24.39	gi|16716569	protease, serine, 1 [Mus musculus]	5
15	19.59	gi|114145561	keratin, type II cytoskeletal 8 [Mus musculus]	1
16	9.61	gi|22164776	keratin, type II cytoskeletal 79 [Mus musculus]	1
17	3.70	gi|172072677	urocanate hydratase [Mus musculus]	1
18	10.36	gi|7949055	hippocalcin-like protein 1 [Mus musculus]	1
19	9.39	gi|30424792	inactive hydroxysteroid dehydrogenase-like protein 1 [Mus musculus]	0
20	15.45	gi|6678439	anionic trypsin-2 precursor [Mus musculus]	2
21	5.74	gi|31981920	ftsJ methyltransferase domain-containing protein 1 [Mus musculus]	0
22	6.36	gi|124486710	DENN domain-containing protein 3 [Mus musculus]	0
23	10.59	gi|126157504	serine/arginine repetitive matrix protein 2 [Mus musculus]	0

The most abundant 23 proteins bound to/eluted from the PST affinity column are displayed, as well as the number of peptides identified in each protein. Peptides from the trypsin-digested SDS-PAGE protein band were analyzed by nano-LC-nano-ESI MS/MS, and then identified with Protein Pilot software.
doi:10.1371/journal.pone.0084132.t001

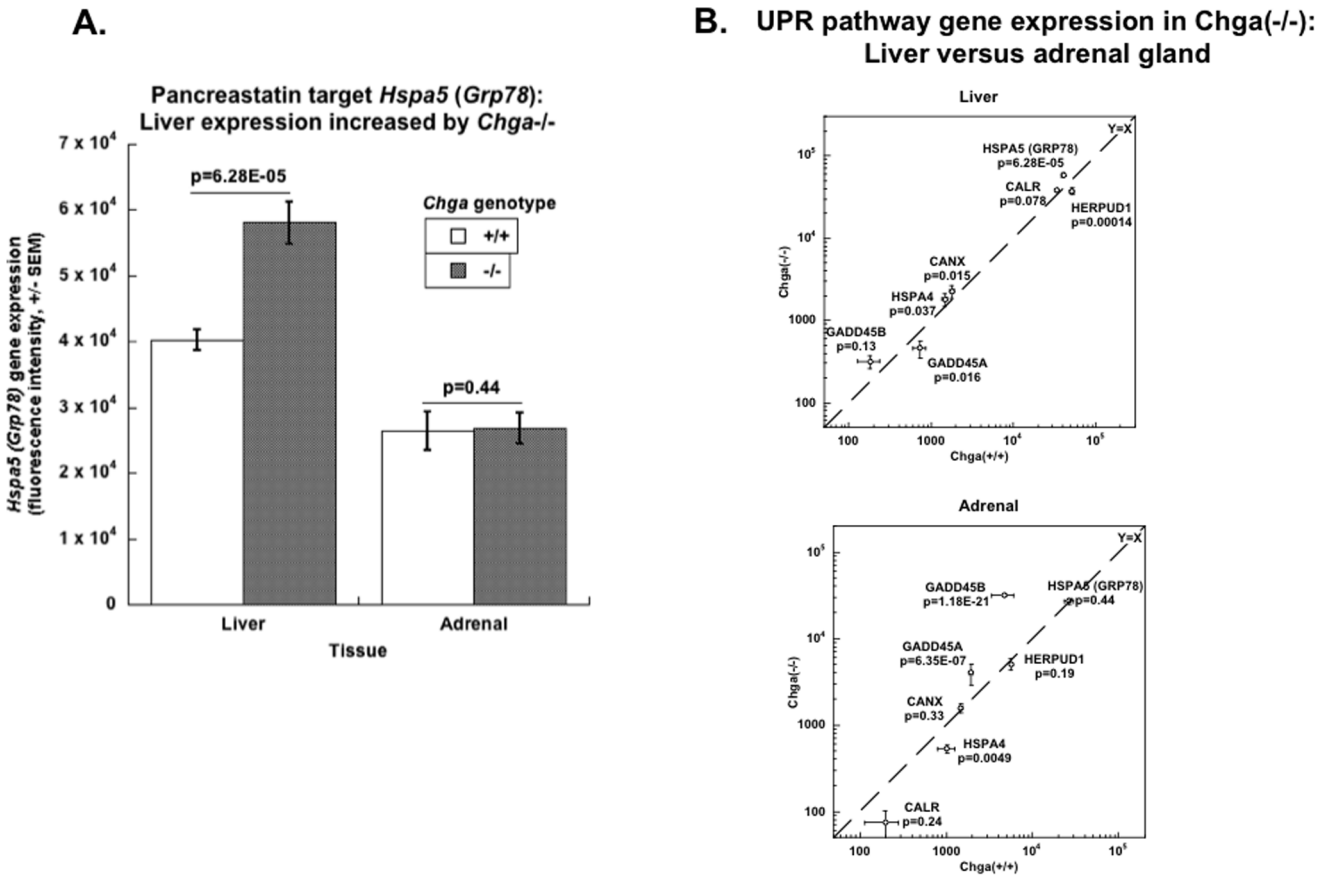

Figure 2. Expression of GRP78 and other UPR pathway genes in liver and adrenal transcriptomes of mice without CHGA (−/−). (**A**) **Liver and adrenal gland expression of GRP78** in CHGA(−/−) mice compared to wild-type (WT, +/+). (**B**) **Expression of UPR pathway genes** in liver (upper panel) and adrenal gland (lower panel).
doi:10.1371/journal.pone.0084132.g002

p = 7.98E-128, Benjamini p = 7.98E-128 (sic), and FDR = 2.07E-127. Selected UPR components are plotted in Fig. 2B.

Almost every heat shock family transcript (Figure 3A) on the chip was also significantly differentially expressed in mouse liver such that −/− > +/+: HSPA9 (−18%, p = 0.014), HSBP1 (+19%, p = 0.047), HSP90AB1 (+19%, p = 0.030; two probes), HSPA4 (+23%, p = 0.0.037), HSPA8 (+38%, p = 0.00033; 3 probes), HSP110 (+39%, p = 0.00097), HSP90AA1 (+25%, p = 0.0088; 2 probes), HSF4 (+63%, p = 0.037), HSPA1B (+147%, p = 2.80E-15; 3 probes), HSPA1A (+814%, p = 0.023).

Pro-apoptotic transcripts (Figure 3B) were globally expressed differentially in mouse liver, but this time as −/− > +/+: CASP6 (−28%, p = 0.00023), Bcl2l11 (−34%, p = 1.3000e-05), Bclaf1 (−32%, p = 7.6300e-05), BID (−50%, p = 5.6500e-06), Bcl2l1 (−44%, p = 0.04), Bcl2l2 (−58%, p = 0.04), Bcl2l10 (−82%, p = 0.04), Dido1 (−22%, p = 0.0082), DAXX (−24%, p = 0.015).

PST unexpectedly *inhibits* the ATPase enzymatic activity of GRP78, as well its transcription

ATP binding and hydrolysis are essential for the chaperone activity of HSP70-family proteins; thus the UPR-adaptive effect of GRP78 is dependent on its functional ATP binding domain. HSP70s bind ATP with high affinity, and their ATPase activity, stimulated by binding to the unfolded protein, catalyzes re-folding. Indeed, we found that GRP78, over a range of concentrations, yielded an increase in A_{620} as evidence of liberated free phosphate (Pi; Fig. 4A). However, PST (at 1 or 10 μM) displayed a significant *inhibitory* effect (~25% and ~60% respectively) on the ATPase activity of GRP78 (Fig. 4B). The IC_{50} for this inhibition was estimated at ~5.2 μM (Fig. 4B).

To test the effect of PST on GRP78 *expression*, we used a plasmid containing the GRP78 promoter region driving a luciferase reporter. Basal promoter activity did not change with PST, but PST substantially (by ~32%) *inhibited* up-regulation of the GRP78 promoter during UPR activation by tunicamycin (Fig. 4C).

PST alters glucose metabolism and insulin action

In 3T3-L1 adipocytes, we found a ~30% inhibition of insulin-stimulated glucose uptake by PST (Fig. 5A). To gain a better understanding of PST's role in glucose release, we transfected HepG2 hepatocytes with a G6Pase promoter/luciferase reporter plasmid, since G6Pase catalyzes the final step in both gluconeogenesis and glycogenolysis, resulting the formation of glucose plus free phosphate from glucose-6-phosphate. G6Pase expression was *up-regulated* ~1.4-fold by PST (Fig. 5B). Insulin suppressed PST-induced activation of the G6Pase promoter by ~40% (Fig. 5B).

PST inhibition of GRP78 ATPase enzymatic activity stimulates transcription of the gluconeogenic/glycogenolytic enzyme G6Pase

Since G6Pase is involved in the final step of both gluconeogenesis and glycogenolysis, we tested the effect of GRP78 as well as

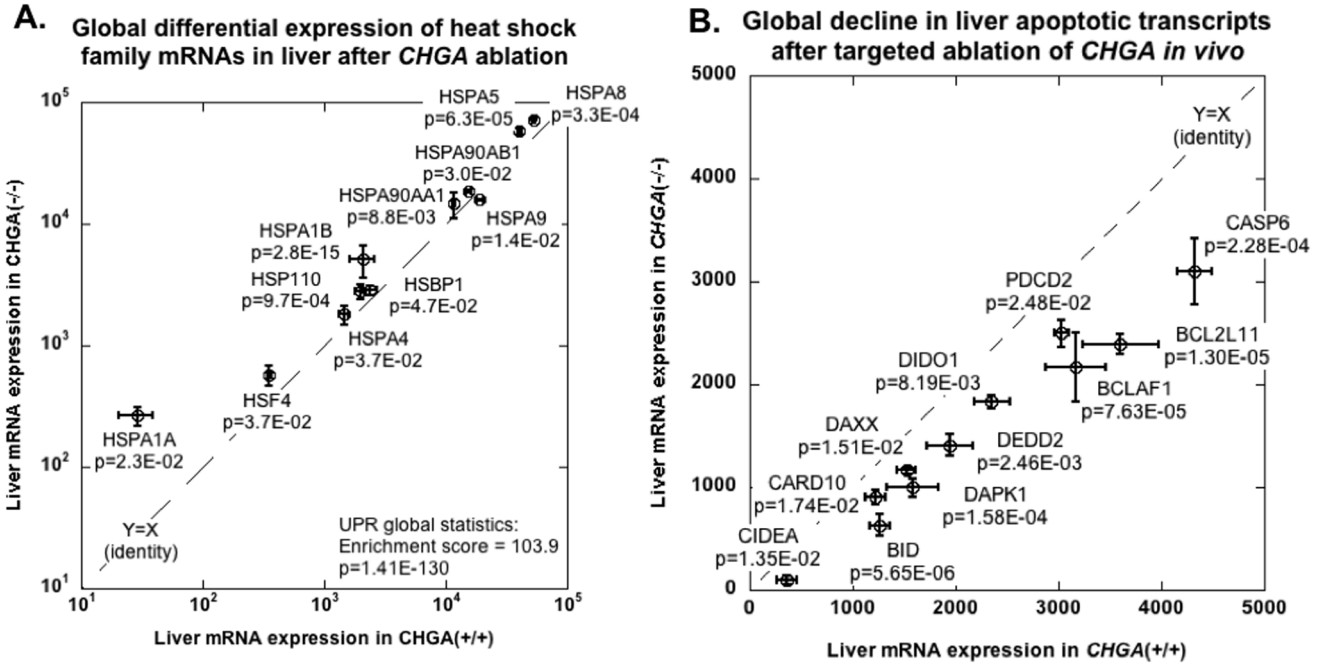

Figure 3. Expression of adaptive (heat shock family) and pro-apoptotic UPR genes in liver transcriptome of mice with systemic deletion of the CHGA gene. Transcripts were from the top 1000 most differentially expressed liver mRNAs (in −/− versus +/+ mice). (**A**) **Liver expression of heat shock family transcripts.** Each transcript was differentially expressed across the strains, with 10 of 11 transcripts *over*-expressed in −/− mice, and one under-expressed. Chi-square = 5.87, P = 0.0154. (**B**) **Liver expression of pro-apoptotic transcripts**. There was global *under*-expression of pro-apoptotic transcripts. Chi-square = 9.17, P = 0.0025.
doi:10.1371/journal.pone.0084132.g003

UPR activation on G6Pase expression (Figure 6A). In this system, PST augmented G6Pase expression by ~45%; during UPR activation or GRP78 addition, basal G6Pase expression declined by ~22–24%, and the PST-induced increment was abolished. As internal controls, at the protein level, activation of the hepatocyte UPR (by tunicamycin or thapsigargin) resulted in a ~15-fold increase in GRP78 protein expression as compared to untreated cells (Fig. 6C), while in cells co-transfected with a GRP78-expression plasmid, a moderate (~2-fold) increase in GRP78 protein expression was observed.

To further clarify how GRP78 affects G6Pase expression, we used adenosine-derived compounds that bind to and inhibit the GRP78 ATPase domain: VER-155008 and adenosine 5′-diphosphate (ADP). With either VER-155008 or ADP addition, basal G6Pase-luciferase promoter activity rose (Fig. 6B) to a level comparable to PST activation. Again, over-expression of GRP78 reduced G6Pase promoter activity, though inhibition of GRP78 ATPase activity by PST, VER-155008 or ADP could not fully overcome the effect of GRP78 over-expression.

Discussion

Overview

To identify potential target proteins for PST action, we used ligand affinity chromatography with biotinylated human PST ($hCgA_{273–301}$-amide) as "bait" on a murine liver homogenate (as "prey"), and found that PST interacts in pH-dependent fashion with GRP78. GRP78 (also known as HSPA5 or BIP) belongs to a group of heat shock proteins (or chaperones) playing a role in folding and assembly of nascent and malfolded proteins in the lumen of the endoplasmic reticulum (ER) [32].

In stressful conditions such as accumulation of misfolded proteins, the capacity of these chaperones may become inadequate, leading to a condition defined as "ER stress". The cellular response to ER stress, referred to as the Unfolded Protein Response (UPR), activates signaling pathways from three ER stress sensors: Inositol-Requiring protein 1 (IRE1α), PKR-like ER Kinase (PERK) and Activation Transcription Factor 6 (ATF6). The actions of these signaling cascades serve to reduce ER stress through induction of chaperones and attenuation of protein translation.

Overall GRP78 balance within the cell is thus critical for secretory pathway homeostasis (the adaptive UPR) and avoidance of programmed cell death (the pro-apoptotic UPR) [33]. GRP78 has been associated with dysglycemic disease states as well as glucose metabolism in several ways [34–36]. Previous studies have shown that ER stress may impair insulin action in adipocytes and hepatocytes, as well as reduce insulin secretion from pancreatic islet beta cells; in such settings, a relative deficit in the UPR may play a causal role in the development of type 2 diabetes [37–39]. Indeed, haploinsufficiency of GRP78 attenuates diet-induced obesity and insulin resistance in the GRP78(+/−) heterozygote mouse [40].

ER stress and induction of the UPR

Induction of GRP78 biosynthesis by ER stress is mediated by multiple copies of the ER stress response element (ERSE) [41,42], through which both ATF6 and XBP1 activate GRP78 transcription. Insulin and IGF-1 can regulate GRP78 expression and augment the adaptive capacity of the UPR under ER stress conditions [43–48]. Although GRP78 expression is a downstream target of insulin [43], recent evidence suggests that GRP78 and the other adaptive ER chaperone proteins regulate organismal insulin sensitivity and glucose homeostasis [35,36,49,50], in addition to protecting cells during acute stress.

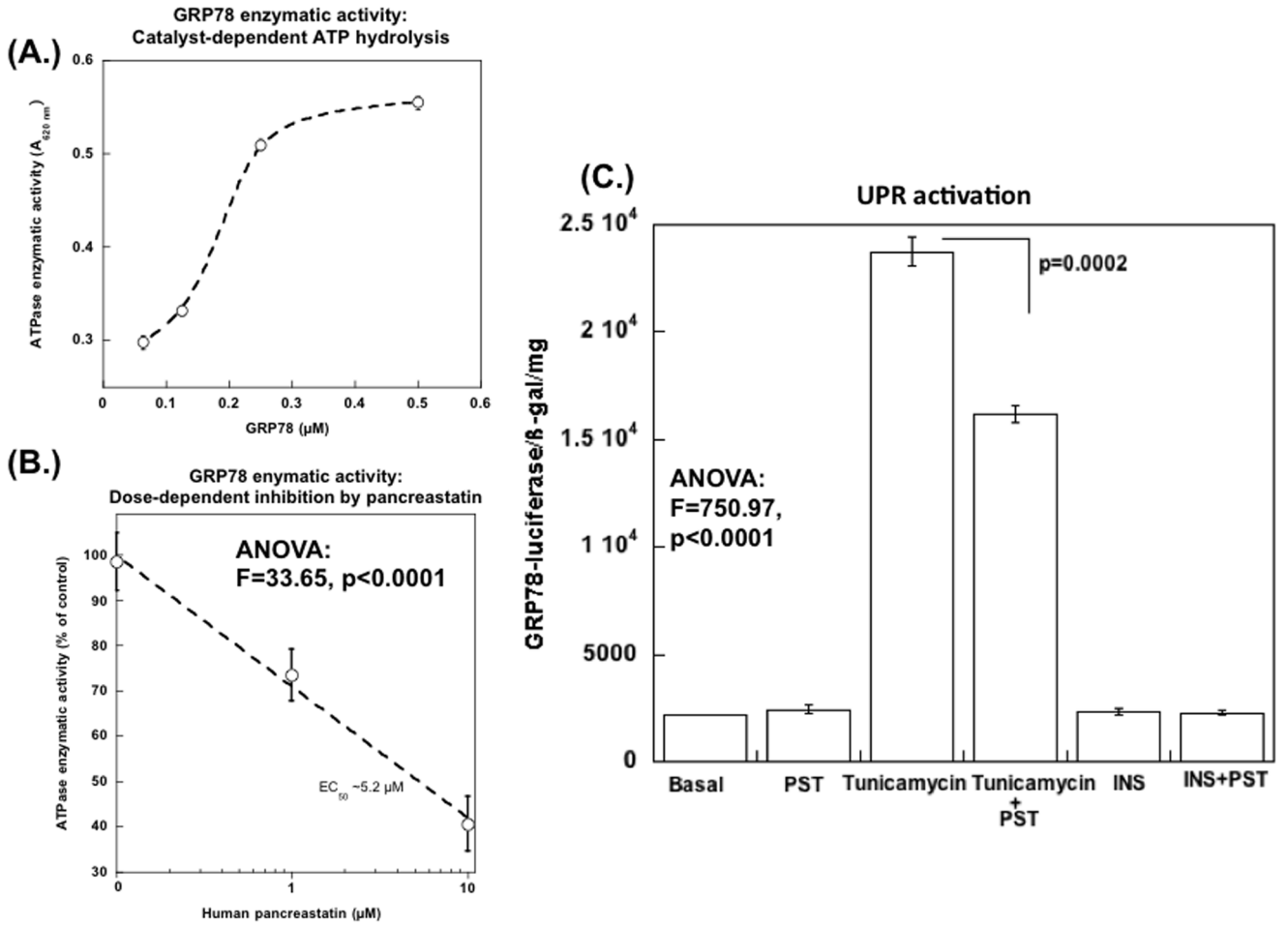

Figure 4. Pancreastatin *inhibits* the ATPase enzymatic activity of GRP78, as well as its transcription. (**A**) **ATPase enzymatic activity of GRP78** (concentration-dependent, steady-state) was measured as an increase in A_{620} (liberated as free phosphate, Pi) using 0.063, 0.125, 0.25 or 0.5 μM GRP78 in 50 μl of assay buffer, as described in experimental procedures. (**B**) **PST *inhibition* of the ATPase enzymatic activity of GRP78**. ATPase activity was measured in the presence of 0, 1, or 10 μM PST: IC_{50} of PST inhibition (by interpolation). (**C**) **GRP78 gene expression: *Inhibition* by PST**. Human HepG2 hepatocytes were transfected with GRP78 promoter driving a luciferase reporter along with beta Gal reporter plasmid and 5 hrs after transfection cells were treated with tunicamycin (5 μg/mL) in the presence or absence of PST (100 nM). Cells were harvested after 18–20 hrs for measurement of luciferase activity, beta gal activity and protein.
doi:10.1371/journal.pone.0084132.g004

Genetic ablation of CHGA in the mouse leads to global over-expression of not only GRP78 (Fig. 2A) but also other heat shock transcripts in liver (Fig. 3A), while PST itself down-regulates GRP78 activity and synthesis (Fig. 4B & C). The UPR may subserve both adaptive (stress-survival) and pro-apoptotic (programmed cell death) outcomes [51]; within the UPR, heat shock proteins (HSPs) are largely adaptive (i.e., pro-survival in the face of stress). Pro-apoptotic transcripts were globally down-regulated in CHGA(−/−) mouse liver (Fig. 3B). CHGA(−/−) mice also display improved glycemia with enhanced insulin sensitivity *in vivo* [23]. The observation that activation of the adaptive UPR leads to enhanced insulin sensitivity with decreased obesity has been described previously [40].

Role of GRP78 and its ATPase enzymatic activity

As a member of the HSP70 family, the molecular chaperone GRP78 (BIP, HSPA5) is involved in several cellular processes, including regulation of calcium homoeostasis, translocation of newly synthesized polypeptides across the endoplasmic reticulum membrane and their subsequent folding, maturation and transport. HSP70-group proteins harbor two functional domains: a ~44 kDa amino-terminal domain possesses ATPase activity, while a carboxyl-terminal domain consists of a ~20 kDa peptide-binding subdomain, followed by a helical and variable ~10 kDa carboxyl-terminal tail. GRP78 and other HSP70 proteins self-associate into multiple oligomeric forms, and the binding of an unfolded peptide substrate onto the carboxyl-terminal domain (or binding of ATP onto the amino-terminal domain) promotes depolymerization and stabilization of the GRP78 monomer [52].

GRP78 contacts a variety of proteins in the secretory pathway, such as the luminal "J" domain of the transmembrane protein MTJ1, thereby stimulating GRP78's ATPase enzymatic activity, as an energetic source for the re-folding process [53].

In contrast to such characteristic *activation* of chaperone ATPase enzymatic activity, we observed *inhibition* of GRP78's ATPase activity by PST (Fig. 4B). PST as well as other ATPase inhibitors (VER, ADP) activated G6Pase expression (Fig. 6B, left), suggesting that such GRP78 ATPase inhibition may be central to the dysglycemic effects of PST.

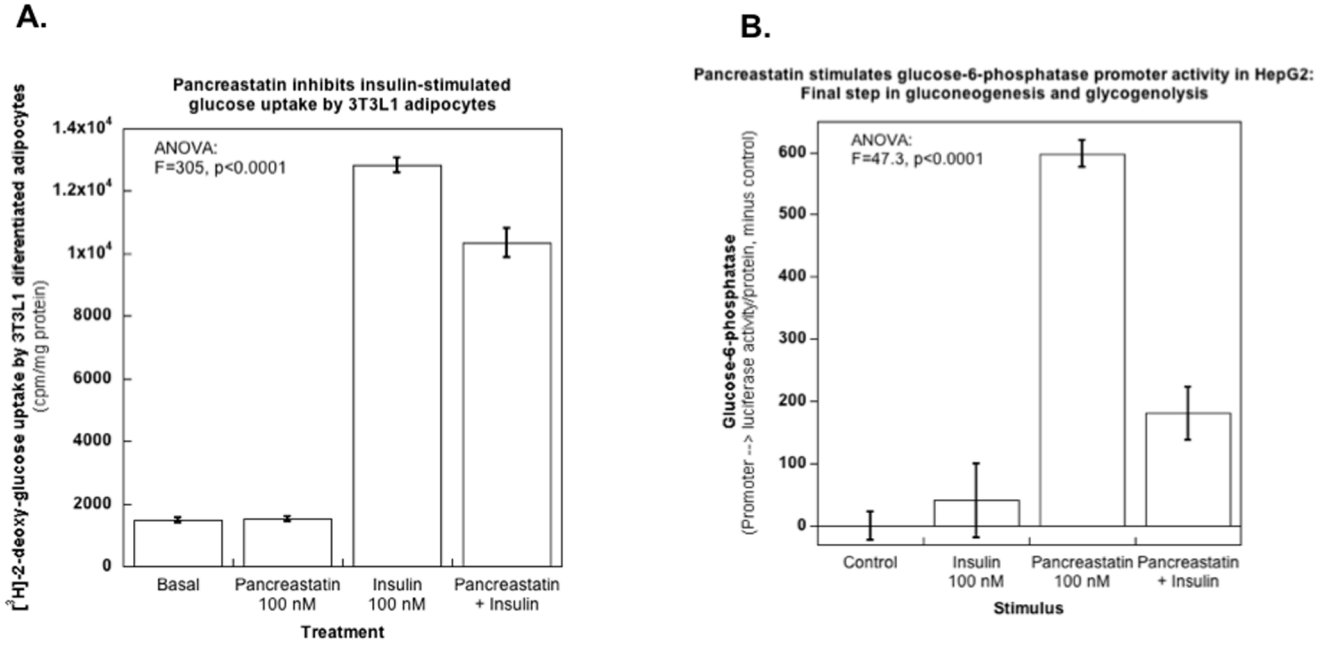

Figure 5. PST acts on both *uptake* and *mobilization* steps for glucose: Effects on cellular glucose metabolism and insulin action. (**A**) **PST and glucose *uptake***. Mouse 3T3-L1 cells were induced to differentiate into adipocytes, and 7–10 days post-differentiation glucose uptake was measured by incubating cells with 2-deoxy-[^{3}H]-glucose in the presence or absence of PST (100 nM), insulin (100 nM), or insulin plus PST (100 nM each). (**B**) **Glucose *mobilization* and PST**: Effects on expression of the gluconeogenic/glycogenolytic enzyme G6Pase (glucose-6-phosphatase). Human HepG2 hepatocytes were transfected with a glucose-6-phosphatase (G6P-ase)→luciferase reporter plasmid along with a beta gal reporter plasmid as mentioned in the experimental procedures, and 5 hrs after transfection cells were treated with PST (100 nM), insulin (100 nM), or both insulin and PST (100 nM each). Cells were harvested at 18–20 hrs after transfection to measure luciferase activity, beta gal activity and protein.
doi:10.1371/journal.pone.0084132.g005

GRP78 over-expression *reduced* G6Pase promoter activity (Fig. 6B, right), reinforcing the diametrically opposing effects of PST and GRP78 on the final step in the gluconeogenic/glycogenolytic cascades (Fig. 6A). The reduction in G6Pase expression by GRP78 over-expression could still be partially reversed by inhibitors of GRP78 ATPase activity (PST, VER-155008, ADP; Fig. 6B, right).

Hepatocytes, glucose, and PST

Obesity, type-2 diabetes, and the associated hepatic steatosis are metabolic disorders characterized by insulin resistance. ER stress activation in the setting of the metabolic syndrome is extensively documented, and chaperone balance may regulate insulin sensitivity and glucose homeostasis [35,36,49,50].

GRP78 protein expression is decreased in liver of obese/diabetic db/db (leptin receptor-deficient) mice, suggesting that the UPR response to ER stress may be defective [54]. In the same db/db model, administration of the chemical chaperones 4-phenylbutyric acid (PBA) or TUDCA (tauroursodeoxycholic acid) reduced ER stress, with restored glucose homeostasis and improved insulin sensitivity [38].

Similarly, adenovirus-mediated short-term GRP78 *over*-expression reduced hepatic steatosis and improved insulin sensitivity in db/db mice [55]. In contrast, long-term GRP78 *under*-expression in heterozygous (+/−) GRP78 knockout mice conferred protection from obesity and insulin resistance after exposure to high-fat diet [40]; in that study, high fat diet activated other chaperones of the adaptive UPR, thereby improving ER quality control and perhaps contributing to metabolic protection.

We established insulin counter-regulatory effects of PST in 3T3-L1 adipocytes and HepG2 hepatocytes (Fig. 5A & 5B), wherein PST inhibits insulin-stimulated glucose uptake while activating the promoter of the gluconeogenic/glycogenolytic enzyme G6Pase. G6Pase expression is ultimately regulated by a number of hormones and metabolites, including insulin, glucagon, glucose, and glucocorticoids [56].

Advantages and limitations of this study

Here we report a novel interacting partner of the dysglycemic PST fragment of CHGA, identifying the UPR chaperone GRP78 (HSPA5, BIP). The binding was pH-dependent, verified by numerous diagnostic peptides on LC-tandem-MS/MS (Figure 1, Table 1, Table S1), and had functional consequences in inhibition of GRP78's ATPase enzymatic activity (Figure 4B).

While previous reports have emphasized potential signaling pathways for PST [23], we can now propose a specific molecule as the PST target that initiates its cascade of metabolic events. Future studies regarding PST's interaction with GRP78 and subsequent cell signaling should benefit our understanding of the pathophysiology of insulin resistance.

Nonetheless, unanswered questions remain. For example, exactly how (and by what pathway) does PST's inhibition of GRP78's ATPase enzymatic activity eventuate in G6Pase activation and consequent dysglycemia?

How might circulating PST contact GRP78, which typically exhibits an intra-cellular location within the ER? A cell surface (plasma membrane) form of GRP78 has been described, especially on cells undergoing the ER stress response as well as on cancer cells [57,58]. Indeed, cell surface GRP78 has been demonstrated to act as a receptor, and several peptides up-regulated in cancer can bind to cell surface GRP78 and thereby influence cell proliferation [59–63]. Some studies have implicated AKT

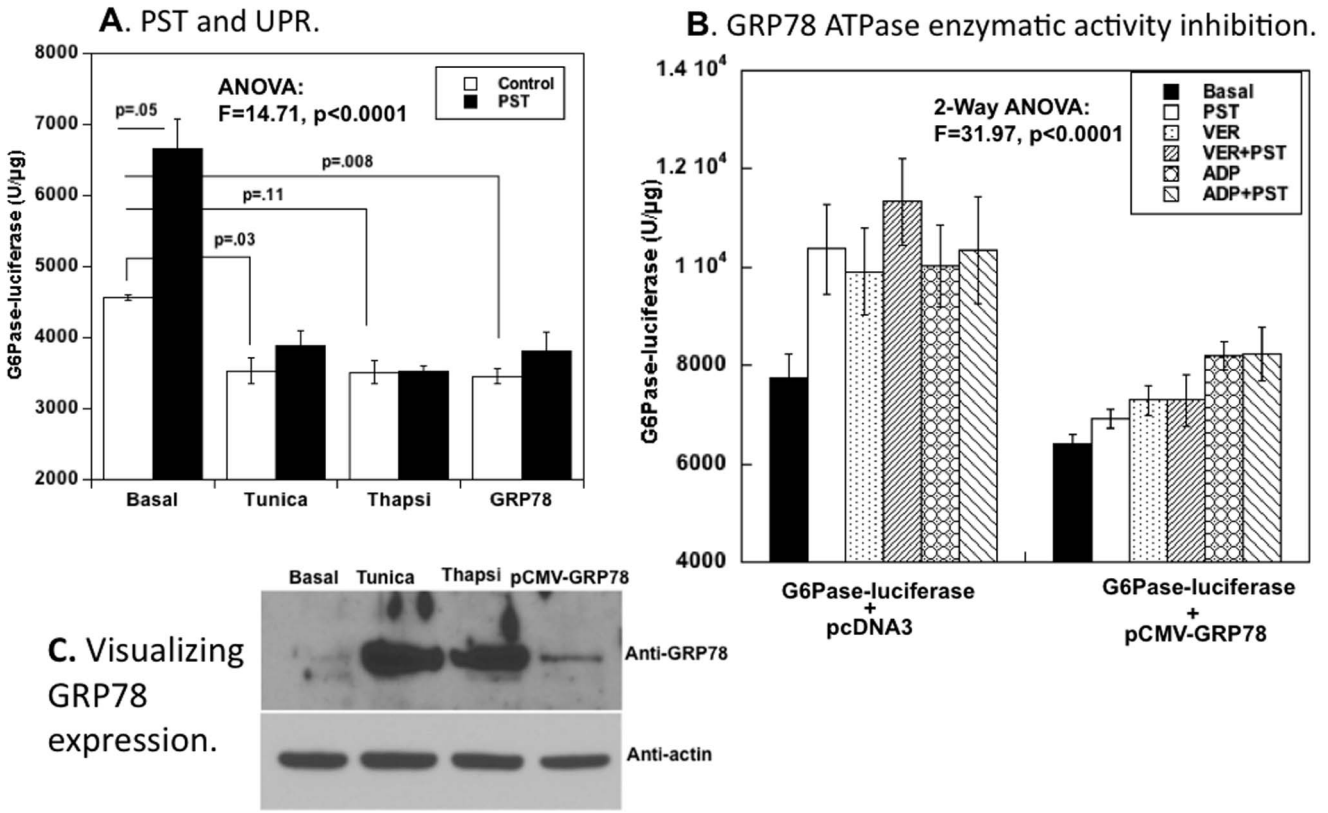

Figure 6. Role of the gluconeogenic/glycogenolytic enzyme G6Pase: Response to PST, GRP78, and inhibition of GRP78's ATPase enzymatic activity. (**A**) **G6Pase expression, PST, and GRP78**. Human HepG2 hepatocytes were transfected with G6P-ase→luciferase, along with pCMV-GRP78 or an empty vector (pCMV promoter without insert). 5 hrs after transfection, cells were treated with PST (100 nM) itself (versus mock), or by UPR activation (tunicamycin, 5 µg/mL; or thapsigargin, 0.3 µM). Cells were harvested at 18–20 hrs to measure luciferase activity and protein. (**B**) **G6Pase expression during ATPase enzymatic activity inhibition of GRP78**. Human HepG2 hepatocytes were transfected as in (A), and 5 hrs later were treated with the GRP78 ATPase inhibitors VER-155008 (1 µM), ADP (10 µM), or PST (100 nM). Cells were harvested at 18–20 hrs to measure luciferase activity and protein. (**C**) **GRP78 expression: Visualization by immunoblot**. Changes in GRP78 expression are shown by anti-GRP78 immunoblot (control: anti-actin), during either UPR activation (by thapsigargin 0.3 µM or tunicamycin 5 µg/mL), or exogenous over-expression (transfection of pCMV-GRP78).
doi:10.1371/journal.pone.0084132.g006

activation in cell surface GRP78 signaling [61,63], a downstream pathway of insulin signaling. We have not explored a specific role of cell surface GRP78. The GRP78va [31] splice variant isoform of GRP78 is another potential target of PST, but the GRP78va isoform seems to be predominantly cytosolic, and analysis of the identified GRP78 peptide fragments (Figure 1B, Table S1) indicated that the PST binding partner was GRP78 itself (rather than GRP78va).

Is there more than one PST receptor? Previous studies on circulating pancreatatin indicate a concentration of ~5–30 pM in

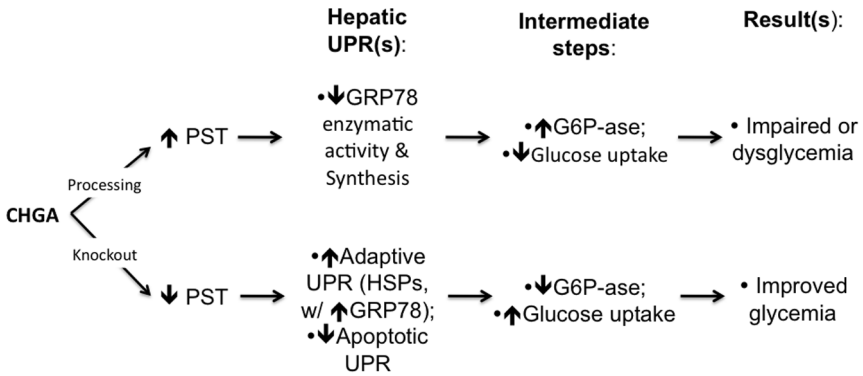

Figure 7. The CHGA dysglycemic fragment pancreastatin (PST): Interactions with GRP78 and the hepatic UPR(s) to achieve metabolic effects. The diagram is presented as a hypothetical schema integrating the experimental results.
doi:10.1371/journal.pone.0084132.g007

humans [64], with effects demonstrable on forearm glucose uptake at ~200 nM, and glucose uptake inhibitory effects on adipocytes with IC_{50} values of ~0.6 nM. Gayen et al [23] also found effects of PST on hepatocytes and adipocytes at 10–100 nM PST. By contrast, we found here that PST inhibited GRP78's ATPase enzymatic activity at IC_{50}~5.2 μM (Fig. 4). Thus, it is conceivable that additional, higher-affinity PST receptors exist. However, we detected no evidence of a PST GPCR during ligand-affinity experiments (Table 1).

Conclusions and perspectives

Since CHGA is released along with catecholamines during sympatho-chromaffin activity, especially under stressful conditions, the PST fragment of CHGA may thus play a role in the pathophysiology of organismal stress by regulating the supply of glucose (and hence energy) to multiple tissues. Under resting circumstances, such actions on glucose metabolism may prove to be deleterious. In Fig. 7, we present a schema integrating our experimental results into a model for PST action via GRP78 and the ER stress pathway. We propose that identification of a novel binding target for ~μM range PST concentrations may advance our understanding of glycemic control, and provide a new avenue of investigation into pathways subserving dysglycemia.

Supporting Information

Table S1 List of peptides identified during MS/MS by Protein Pilot software. Sheet 1 for GRP78 (HSPA5, BIP), sheet 2 for stress 70 protein (GRP75, HSPA9) and sheet 3 for heat shock cognate 71 kDa protein (HSPA8). N represents the rank of the specified protein relative to all other proteins detected. A measure of the protein confidence for a detected protein in terms of ProtScore (either unused or total) and three different measures of % coverage [% Cov, % Cov (50) and % Cov (95)] are shown. (XLSX)

Author Contributions

Conceived and designed the experiments: NB DTO. Performed the experiments: NB RSF JG GB. Analyzed the data: NB RSF DTO. Contributed reagents/materials/analysis tools: SKM. Wrote the paper: NB DTO.

References

1. Sanchez-Margalet V, Gonzalez-Yanes C, Najib S, Santos-Alvarez J (2010) Reprint of: Metabolic effects and mechanism of action of the chromogranin A-derived peptide pancreastatin. Regulatory peptides 165: 71–77.
2. Hakanson R, Ding XQ, Norlen P, Chen D (1995) Circulating pancreastatin is a marker for the enterochromaffin-like cells of the rat stomach. Gastroenterology 108: 1445–1452.
3. Schmidt WE, Siegel EG, Kratzin H, Creutzfeldt W (1988) Isolation and primary structure of tumor-derived peptides related to human pancreastatin and chromogranin A. Proceedings of the National Academy of Sciences of the United States of America 85: 8231–8235.
4. Tamamura H, Ohta M, Yoshizawa K, Ono Y, Funakoshi A, et al. (1990) Isolation and characterization of a tumor-derived human protein related to chromogranin A and its in vitro conversion to human pancreastatin-48. European journal of biochemistry/FEBS 191: 33–39.
5. Kitayama N, Tateishi K, Funakoshi A, Miyasaka K, Shimazoe T, et al. (1994) Pancreastatin molecular forms in normal human plasma. Life sciences 54: 1571–1578.
6. Sanchez-Margalet V, Lucas M, Goberna R (1996) Pancreastatin: further evidence for its consideration as a regulatory peptide. Journal of molecular endocrinology 16: 1–8.
7. Tatemoto K, Efendic S, Mutt V, Makk G, Feistner GJ, et al. (1986) Pancreastatin, a novel pancreatic peptide that inhibits insulin secretion. Nature 324: 476–478.
8. Ostenson CG, Sandler S, Efendic S (1989) Effects of porcine pancreastatin on secretion and biosynthesis of insulin and glucose oxidation of isolated rat pancreatic islets. Pancreas 4: 441–446.
9. Sanchez-Margalet V, Gonzalez-Yanes C, Santos-Alvarez J, Najib S (2000) Pancreastatin. Biological effects and mechanisms of action. Advances in experimental medicine and biology 482: 247–262.
10. Sanchez-Margalet V, Calvo JR, Goberna R (1992) Glucogenolytic and hyperglycemic effect of 33-49 C-terminal fragment of pancreastatin in the rat in vivo. Hormone and metabolic research = Hormon- und Stoffwechselforschung = Hormones et metabolisme 24: 455–457.
11. Sanchez V, Calvo JR, Goberna R (1990) Glycogenolytic effect of pancreastatin in the rat. Bioscience reports 10: 87–91.
12. Sanchez-Margalet V, Gonzalez-Yanes C (1998) Pancreastatin inhibits insulin action in rat adipocytes. The American journal of physiology 275: E1055–1060.
13. Gonzalez-Yanes C, Sanchez-Margalet V (2001) Pancreastatin, a chromogranin-A-derived peptide, inhibits insulin-stimulated glycogen synthesis by activating GSK-3 in rat adipocytes. Biochemical and biophysical research communications 289: 282–287.
14. O'Connor DT, Cadman PE, Smiley C, Salem RM, Rao F, et al. (2005) Pancreastatin: multiple actions on human intermediary metabolism in vivo, variation in disease, and naturally occurring functional genetic polymorphism. The Journal of clinical endocrinology and metabolism 90: 5414–5425.
15. Sanchez-Margalet V, Valle M, Goberna R (1994) Receptors for pancreastatin in rat liver membranes: molecular identification and characterization by covalent cross-linking. Molecular pharmacology 46: 24–29.
16. Sanchez-Margalet V, Gonzalez-Yanes C, Santos-Alvarez J, Najib S (2000) Characterization of pancreastatin receptor and signaling in rat HTC hepatoma cells. European journal of pharmacology 397: 229–235.
17. Gonzalez-Yanes C, Santos-Alvarez J, Sanchez-Margalet V (1999) Characterization of pancreastatin receptors and signaling in adipocyte membranes. Biochimica et biophysica acta 1451: 153–162.
18. Gonzalez-Yanes C, Santos-Alvarez J, Sanchez-Margalet V (2001) Pancreastatin, a chromogranin A-derived peptide, activates Galpha(16) and phospholipase C-beta(2) by interacting with specific receptors in rat heart membranes. Cellular signalling 13: 43–49.
19. Santos-Alvarez J, Sanchez-Margalet V (2000) Affinity purification of pancreastatin receptor-Gq/11 protein complex from rat liver membranes. Archives of biochemistry and biophysics 378: 151–156.
20. Santos-Alvarez J, Sanchez-Margalet V (1999) G protein G alpha q/11 and G alpha i1,2 are activated by pancreastatin receptors in rat liver: studies with GTP-gamma 35S and azido-GTP-alpha-32P. Journal of cellular biochemistry 73: 469–477.
21. Sanchez-Margalet V, Goberna R (1994) Pancreastatin activates pertussis toxin-sensitive guanylate cyclase and pertussis toxin-insensitive phospholipase C in rat liver membranes. Journal of cellular biochemistry 55: 173–181.
22. Sanchez-Margalet V, Lucas M, Goberna R (1994) Pancreastatin activates protein kinase C by stimulating the formation of 1,2-diacylglycerol in rat hepatocytes. The Biochemical journal 303 (Pt 1): 51–54.
23. Gayen JR, Saberi M, Schenk S, Biswas N, Vaingankar SM, et al. (2009) A novel pathway of insulin sensitivity in chromogranin A null mice: a crucial role for pancreastatin in glucose homeostasis. The Journal of biological chemistry 284: 28498–28509.
24. Sanchez-Margalet V, Lobon JA, Gonzalez A, Fernandez-Soto ML, Escobar-Jimenez F, et al. (1998) Increased plasma pancreastatin-like levels in gestational diabetes: correlation with catecholamine levels. Diabetes care 21: 1951–1954.
25. Sanchez-Margalet V, Valle M, Lobon JA, Escobar-Jimenez F, Perez-Cano R, et al. (1995) Plasma pancreastatin-like immunoreactivity correlates with plasma norepinephrine levels in essential hypertension. Neuropeptides 29: 97–101.
26. Sanchez-Margalet V, Valle M, Lobon JA, Maldonado A, Escobar-Jimenez F, et al. (1995) Increased plasma pancreastatin-like immunoreactivity levels in non-obese patients with essential hypertension. Journal of hypertension 13: 251–258.
27. Funakoshi A, Tateishi K, Shinozaki H, Matsumoto M, Wakasugi H (1990) Elevated plasma levels of pancreastatin (PST) in patients with non-insulin-dependent diabetes mellitus (NIDDM). Regulatory peptides 30: 159–164.
28. Ni M, Lee AS (2007) ER chaperones in mammalian development and human diseases. FEBS letters 581: 3641–3651.
29. Shevchenko A, Wilm M, Vorm O, Mann M (1996) Mass spectrometric sequencing of proteins silver-stained polyacrylamide gels. Analytical chemistry 68: 850–858.
30. Friese RS, Gayen JR, Mahapatra NR, Schmid-Schonbein GW, O'Connor DT, et al. (2010) Global metabolic consequences of the chromogranin A-null model of hypertension: transcriptomic detection, pathway identification, and experimental verification. Physiological genomics 40: 195–207.
31. Ni M, Zhou H, Wey S, Baumeister P, Lee AS (2009) Regulation of PERK signaling and leukemic cell survival by a novel cytosolic isoform of the UPR regulator GRP78/BiP. PloS one 4: e6868.
32. Rutkowski DT, Kaufman RJ (2004) A trip to the ER: coping with stress. Trends in cell biology 14: 20–28.
33. Garrido C, Gurbuxani S, Ravagnan L, Kroemer G (2001) Heat shock proteins: endogenous modulators of apoptotic cell death. Biochemical and biophysical research communications 286: 433–442.

34. Pfaffenbach KT, Lee AS (2011) The critical role of GRP78 in physiologic and pathologic stress. Current opinion in cell biology 23: 150–156.
35. Eizirik DL, Cardozo AK, Cnop M (2008) The role for endoplasmic reticulum stress in diabetes mellitus. Endocrine reviews 29: 42–61.
36. Flamment M, Kammoun HL, Hainault I, Ferre P, Foufelle F (2010) Endoplasmic reticulum stress: a new actor in the development of hepatic steatosis. Current opinion in lipidology 21: 239–246.
37. Chan JY, Luzuriaga J, Bensellam M, Biden TJ, Laybutt DR (2013) Failure of the adaptive unfolded protein response in islets of obese mice is linked with abnormalities in beta-cell gene expression and progression to diabetes. Diabetes 62: 1557–1568.
38. Ozcan U, Yilmaz E, Ozcan L, Furuhashi M, Vaillancourt E, et al. (2006) Chemical chaperones reduce ER stress and restore glucose homeostasis in a mouse model of type 2 diabetes. Science 313: 1137–1140.
39. Cnop M, Foufelle F, Velloso LA (2012) Endoplasmic reticulum stress, obesity and diabetes. Trends in molecular medicine 18: 59–68.
40. Ye R, Jung DY, Jun JY, Li J, Luo S, et al. (2010) Grp78 heterozygosity promotes adaptive unfolded protein response and attenuates diet-induced obesity and insulin resistance. Diabetes 59: 6–16.
41. Schroder M, Kaufman RJ (2005) The mammalian unfolded protein response. Annual review of biochemistry 74: 739–789.
42. Yoshida H, Haze K, Yanagi H, Yura T, Mori K (1998) Identification of the cis-acting endoplasmic reticulum stress response element responsible for transcriptional induction of mammalian glucose-regulated proteins. Involvement of basic leucine zipper transcription factors. The Journal of biological chemistry 273: 33741–33749.
43. Inageda K (2010) Insulin modulates induction of glucose-regulated protein 78 during endoplasmic reticulum stress via augmentation of ATF4 expression in human neuroblastoma cells. FEBS letters 584: 3649–3654.
44. Ma Y, Brewer JW, Diehl JA, Hendershot LM (2002) Two distinct stress signaling pathways converge upon the CHOP promoter during the mammalian unfolded protein response. Journal of molecular biology 318: 1351–1365.
45. Luo S, Baumeister P, Yang S, Abcouwer SF, Lee AS (2003) Induction of Grp78/BiP by translational block: activation of the Grp78 promoter by ATF4 through and upstream ATF/CRE site independent of the endoplasmic reticulum stress elements. The Journal of biological chemistry 278: 37375–37385.
46. Novosyadlyy R, Kurshan N, Lann D, Vijayakumar A, Yakar S, et al. (2008) Insulin-like growth factor-I protects cells from ER stress-induced apoptosis via enhancement of the adaptive capacity of endoplasmic reticulum. Cell death and differentiation 15: 1304–1317.
47. Winnay JN, Boucher J, Mori MA, Ueki K, Kahn CR (2010) A regulatory subunit of phosphoinositide 3-kinase increases the nuclear accumulation of X-box-binding protein-1 to modulate the unfolded protein response. Nature medicine 16: 438–445.
48. Park SW, Zhou Y, Lee J, Lu A, Sun C, et al. (2010) The regulatory subunits of PI3K, p85alpha and p85beta, interact with XBP-1 and increase its nuclear translocation. Nature medicine 16: 429–437.
49. Ozcan U, Cao Q, Yilmaz E, Lee AH, Iwakoshi NN, et al. (2004) Endoplasmic reticulum stress links obesity, insulin action, and type 2 diabetes. Science 306: 457–461.
50. Nakatani Y, Kaneto H, Kawamori D, Yoshiuchi K, Hatazaki M, et al. (2005) Involvement of endoplasmic reticulum stress in insulin resistance and diabetes. The Journal of biological chemistry 280: 847–851.
51. Chan JY, Cooney GJ, Biden TJ, Laybutt DR (2011) Differential regulation of adaptive and apoptotic unfolded protein response signalling by cytokine-induced nitric oxide production in mouse pancreatic beta cells. Diabetologia 54: 1766–1776.
52. Carlino A, Toledo H, Skaleris D, DeLisio R, Weissbach H, et al. (1992) Interactions of liver Grp78 and Escherichia coli recombinant Grp78 with ATP: multiple species and disaggregation. Proceedings of the National Academy of Sciences of the United States of America 89: 2081–2085.
53. Chevalier M, Rhee H, Elguindi EC, Blond SY (2000) Interaction of murine BiP/GRP78 with the DnaJ homologue MTJ1. The Journal of biological chemistry 275: 19620–19627.
54. Yamagishi N, Ueda T, Mori A, Saito Y, Hatayama T (2012) Decreased expression of endoplasmic reticulum chaperone GRP78 in liver of diabetic mice. Biochemical and biophysical research communications 417: 364–370.
55. Kammoun HL, Chabanon H, Hainault I, Luquet S, Magnan C, et al. (2009) GRP78 expression inhibits insulin and ER stress-induced SREBP-1c activation and reduces hepatic steatosis in mice. The Journal of clinical investigation 119: 1201–1215.
56. Streeper RS, Svitek CA, Goldman JK, O'Brien RM (2000) Differential role of hepatocyte nuclear factor-1 in the regulation of glucose-6-phosphatase catalytic subunit gene transcription by cAMP in liver- and kidney-derived cell lines. The Journal of biological chemistry 275: 12108–12118.
57. Wang M, Wey S, Zhang Y, Ye R, Lee AS (2009) Role of the unfolded protein response regulator GRP78/BiP in development, cancer, and neurological disorders. Antioxidants & redox signaling 11: 2307–2316.
58. Delpino A, Castelli M (2002) The 78 kDa glucose-regulated protein (GRP78/BIP) is expressed on the cell membrane, is released into cell culture medium and is also present in human peripheral circulation. Bioscience reports 22: 407–420.
59. Arap MA, Lahdenranta J, Mintz PJ, Hajitou A, Sarkis AS, et al. (2004) Cell surface expression of the stress response chaperone GRP78 enables tumor targeting by circulating ligands. Cancer cell 6: 275–284.
60. Zhang Y, Liu R, Ni M, Gill P, Lee AS (2010) Cell surface relocalization of the endoplasmic reticulum chaperone and unfolded protein response regulator GRP78/BiP. The Journal of biological chemistry 285: 15065–15075.
61. Misra UK, Deedwania R, Pizzo SV (2006) Activation and cross-talk between Akt, NF-kappaB, and unfolded protein response signaling in 1-LN prostate cancer cells consequent to ligation of cell surface-associated GRP78. The Journal of biological chemistry 281: 13694–13707.
62. Shani G, Fischer WH, Justice NJ, Kelber JA, Vale W, et al. (2008) GRP78 and Cripto form a complex at the cell surface and collaborate to inhibit transforming growth factor beta signaling and enhance cell growth. Molecular and cellular biology 28: 666–677.
63. Misra UK, Pizzo SV (2010) Modulation of the unfolded protein response in prostate cancer cells by antibody-directed against the carboxyl-terminal domain of GRP78. Apoptosis : an international journal on programmed cell death 15: 173–182.
64. O'Connor DT, Cadman PE, Smiley C, Salem RM, Rao F, et al. (2005) Pancreastatin: multiple actions on human intermediary metabolism in vivo, variation in disease, and naturally occurring functional genetic polymorphism. J Clin Endocrinol Metab 90: 5414–5425.